Structural Engineering and Mechanics, *Vol. 68, No. 4 (2018) 497-505*
DOI: https://doi.org/10.12989/sem.2018.68.4.497

PFC3D simulation of the effect of particle size on the single edge-notched rectangle bar in bending test

Hadi Haeri[1], Vahab Sarfarazi[2] and Zheming Zhu*[1]

[1]MOE Key Laboratory of Deep Underground Science and Engineering, School of Architecture and Environment, Sichuan University, Chengdu 610065, China
[2]Department of Mining Engineering, Hamedan University of Technology, Hamedan, Iran

(Received August 2, 2018, Revised September 26, 2018, Accepted October 11, 2018)

Abstract. Three points bending flexural test was modeled numerically to study the crack propagation in the pre-cracked beams. The pre-existing edge cracks in the beam models were considered to investigate the crack propagation and coalescence paths within the modeled samples. The effects of particle size on the single edge-notched round bar in bending test were considered too. The results show that Failure pattern is constant by increasing the ball diameter. Tensile cracks are dominant mode of failure. These crack initiates from notch tip, propagate parallel to loading axis and coalescence with upper model boundary. Number of cracks increase by decreasing the ball diameter. Also, tensile fracture toughness was decreased with increasing the particle size. In the present study, the influences of particles sizes on the cracks propagations and coalescences in the brittle materials such as rocks and concretes are numerically analyzed by using a three dimensional particle flow code (PFC3D). These analyses improve the understanding of the stability of rocks and concretes structures such as rock slopes, tunnel constructions and underground openings.

Keywords: SENRBB test; pre-existing edge cracks; PFC3D

1. Introduction

The process of cracks propagations and cracks coalescences within the rocks and concretes structures under different loading conditions may considerably reduce the strength of such important structures. The crack propagation mechanism in concrete beams and controlling the stability of the concrete structures may involve the serious problems related to the fracture mechanics design of these engineering structures. The three and four-point bending beam specimens are usually tested in the laboratory to investigate the strength and flexural behavior of concrete beams. The tensile strength and the Mode I and Mode II fracture toughness of concrete beams can be determined by preparing some special specimens (Dai *et al.* 2011, Wang *et al.* 2011, Wang *et al.* 2012, Yoshihara 2013, Lancaster *et al.* 2013, Jiang *et al.* 2014, Noel and Soudki 2014). The fracture of asphalt mixtures is studied by Zeng *et al.* (2014) using a damage model mechanism in the beam specimens under three-point bending. The effects of cracks locations the coarse aggregates distribution on the crack propagation paths and damage behavior of the asphalt mixtures were studied. They stated that the simulation results are in good agreement with the corresponding experimental test results. On the other hand, Wang *et al.* (2015) studied the shear deformation in some reinforced concrete beams (RCB) specimens. They considered some low span-effective depth ratios in a multi-angle truss model to predict the diagonal crack angles. They analyzed the bending moment variations along the span and its effects on the diagonal crack angles. However, many experimental and numerical works have been carried out to study the cracks initiations and cracks propagations in many brittle materials due to the pre-existing cracks considering different loading conditions (Freund 1973, Itou 1996, Belytschko *et al.* 1999, Silling 2000, Zhou 2004, Zhou 2004, Zhou 2007, Zhou 2008, Yang *et al.* 2009, Janeiro and Einstein 2010, Yang 2011, Zhou 2012, Cheng-Zhi and Ping 2012, Ameen *et al.* 2011, Leonel *et al.* 2012, Yoshihara 2013, Lancaster *et al.* 2013, Jiang *et al.* 2014, Janeiro and Einstein 2010, Zhou *et al.* 2012, Zhao *et al.* 2013, Lancaster *et al.* 2013, Ramadoss 2013, Zhou 2014, Haeri *et al.* 2014, Zeng *et al.* 2014, Pan *et al.* 2014, Noel and Soudki 2014, Oliveira and Leonel 2014, Mobasher *et al.* 2014, Gerges *et al*. 2015, Tiang *et al.* 2015, Lu *et al.* 2015, Liu *et al.* 2015, Oliaei 2015, Lin 2015, Fan 2015, Zhang 2015, Hofmann 2015, Silva *et al.* 2015, Zhou *et al.* 2015, Yang 2015, Haeri 2015a, b, c, Haeri *et al.* 2015a, b, c, Li *et al.* 2015, Li *et al.* 2016, Li *et al.* 2016, Haeri *et al.* 2016a, b, c, Haeri and Sarfarazi 2016, Sarfarazi *et al.* 2014, Zhou *et al.* 2015, Sarfarazi *et al.* 2016a, b, c, Sarfarazi and Haeri *et al.* 2016, Shuraim 2016, Sardemir 2016, Li *et al.* 2016, Akbas 2016, Rajabi 2016, Yaylac 2016, Fan *et al.* 2016, Mohammad 2016, Zhou 2016, Oetomo 2016, Lee 2016, Shaowei *et al.* 2016, Bi *et al.* 2016, Zhou *et al.* 2016, Wang *et al.* 2017, Silling 2017, Bi *et al.* 2017). Two types of cracks have been identified in these research, wing crack and shear crack. The results show that the wing cracks disappeared by increasing the confining pressure.

*Corresponding author, Professor
E-mail: zhemingzhu@hotmail.com

http://www.techno-press.com/journals/sem&subpage=7 ISSN: 1225-4568 (Print), 1598-6217 (Online)

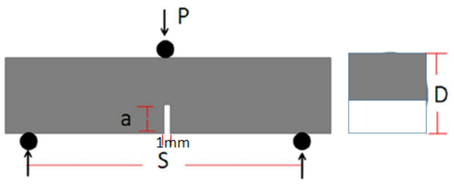

Fig. 1 Schematic diagrams of SENRBB specimen

In the present work, a three dimensional particle flow code (PFC3D) which is based on the versatile discrete element method (DEM) is used to simulate the effects of particle size on the cracks propagations and cracks coalescences in a single edge-notched rectangle bar during the bending test.

1.1 The single edge-notched rectangle bar in bending (SENRBB) specimen

For the SENRBB specimen (Fig. 1), the fracture toughness, *KIC*, is determined using the peak load (*P*), the non-dimensional stress intensity factor, and the specimen dimensions (Ouchterlony 1981). *KIC* may be given as

$$KIC = 0.25\left(\frac{S}{D}\right) YI \frac{F_{max}}{D^{1.5}} \tag{1}$$

Where *YI* is the non-dimensional stress intensity factor, *Fmax* is the maximum load, *S* is the span length between the two support rollers, and *D* is the specimen diameter. The non-dimensional stress intensity factor *YI* is given by

$$YI = 2\left(\frac{D}{S}\right)\left[450.8531P^2\left(\frac{a}{D}\right)^{1.5}\right]/[(a/D) - (a/D)^2]^{0.25} \tag{2}$$

However, in this study, the crack propagation mechanism of concrete specimens is investigated by simulating some flexural tests through a 3D discrete element approach using a sophisticated particle flow code (PFC3D)). The crack initiation and propagation of the preexisting internal cracks is investigated by simulating the three points bending test. The effects of cracks particle size on the specimens fracturing path with in the bridge areas of the samples are studied by this numerical simulation procedure.

2. Numerical simulation

The crack propagation process and cracks coalescences in some single-edge-notched rectangular bars of brittle concretes are being simulated by a three dimensional particle flow code (PFC3D). These simulation procedure is based on the bonded particle modeling approach adopted in most of the discrete element codes.

2.1 Bonded particle model and Particle Flow Code 3D (PFC3D)

A three dimensional discrete element code known as particle flow code (PFC3D) is used to simulate the problem. In this modeling approach, the materials are assumed to be as an assembly of particles bonded to one another at the contact points but each particle can move independently within the assembly (Itasca 1999 version 3.1, Potyondy and Cundall 2004). The explicit finite difference method is used to estimate the interaction forces at the contacts and the particles movements within the assembly. The two models of the contacts that is the linear and non-linear contact models considering the frictional sliding at the particles boundaries are being used in this simulation process. The elastic relationship in between the relative displacements and contact forces of the particles can be modeled by the linear contact modelling procedure. The routines provided by Itasca 1999, Version 3.1, can be used to generate a parallel-bond particle model for PFC3D. This modeling Algorithm may use the following micromechanical properties for the simulation process of the problem i.e. the ball-to ball contact modulus, the stiffness ratio Kn over Ks, the balls coefficient of friction, the parallel normal and shear bonding strengths, the ball radius, the radius multiplier of parallel-bond, the parallel-bond modulus and stiffness ratio. The appropriate micro-properties of the particle assembly are being established through a calibration procedure because the particle contact and the bonding properties cannot be directly determined from the laboratory testing results gained from the actual material samples. The actual material properties gained experimentally from the laboratory tests are the macro properties due to the continuum behavior assumption imposed on the specimens. However, an inverse modeling technique based on the trial and error approach is adopted in PFC3D (Itasca 1999) to determine the appropriate micro mechanical properties of the particle assembly from the macro mechanical properties given by the experimental tests for the numerical simulation of any geo-mechanical problem. In this procedure, the micro mechanical properties are assumed first and the problem is solved for the estimation of the strength and deformation characteristics near to those of macroscopic laboratory results. The procedure is repeated so that the micro mechanical properties values that give a simulated macroscopic response close to those of experimentally obtained values from the laboratory tests. Then, these microscopic properties can be adopted for the numerical simulation of the discontinuous particles or blocks of the simulated material. The limitations of DEM are: (a) Fracture is closely related to the size of elements, and that is so called size effect. (b) Cross effect exists because of the difference between the size and shape of elements with real grains. (c) In order to establish the relationship between the local and macroscopic constitutive laws, data obtained from classical geomechanical tests which may be impractical are used.

2.2 Calibration and preparation of the Brazilian disc model

The calibration of the PFC3D was accomplished by calibrating the tensile strength of the specimen obtained from the Brazilian discs. Four steps were involved to generate a PFC3D material assembly to represent the

Table 1 Micro properties used to represent the intact rock

Parameter	Value	Parameter	Value
Type of particle	disc	Parallel bond radius multiplier	1
Density(kg/m^3)	3000	Young modulus of parallel bond (GPa)	40
Minimum radius (mm)	0.27	Parallel bond stiffness ratio	1.7
Size ratio	1.56	Particle friction coefficient	0.4
Porosity ratio	0.08	Parallel bond normal strength, mean (MPa)	70
Damping coefficient	0.7	Parallel bond normal strength, SD (MPa)	2
Contact young modulus (GPa)	40	Parallel bond shear strength, mean (MPa)	70
Stiffness ratio	1.7	Parallel bond shear strength, SD (MPa)	2

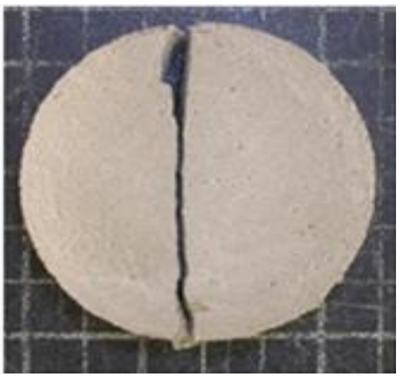

(a)

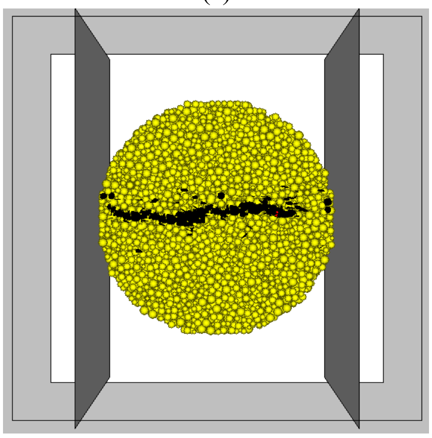

(b)

Fig. 2 failure pattern in (a) physical sample, (b) PFC3D model

Brazilian disc model: (i) generating and packing of the particles, (ii) installing the isotropic stress condition, (iii) eliminating the floating particles, and (iv) installing the particles bonding. The standard calibration process proposed by Potyondy and Cundall (2003) and the micro-properties listed in Table 1 are adopted to calibrate the PFC3D calibration of the particle assembly of the Brazilian disc model. The diameter of the disc was taken as 54 mm and the testing specimen model was made of 15,615 particles. A low speed of 0.016 m/s was used to crush the lateral walls of the disc toward each other to numerically simulate the failure condition of the Brazilian disc. The numerical and experimental failure process of the Brazilian disc samples are shown in Fig. 2(a), Fig. 2(b), respectively.

Table 2 Brazilian tensile strength of physical and numerical samples

Physical tensile strength (MPa)	4.5 and 4.7
Numerical tensile strength (MPa)	4.5

Table 3 The ball size and ball number used in numerical simulation

Ball size(mm)	Ball number	Ball size(mm)	Ball number	Ball size(mm)	Ball number
0.55	55343	1.15	6029	1.75	1761
0.65	38495	1.25	4834	1.85	1491
0.75	22383	1.35	3838	1.95	1273
0.85	18273	1.45	3097	2.05	1096
0.95	11104	1.55	2535	2.15	950
1.05	8157	1.65	2102	2.25	829

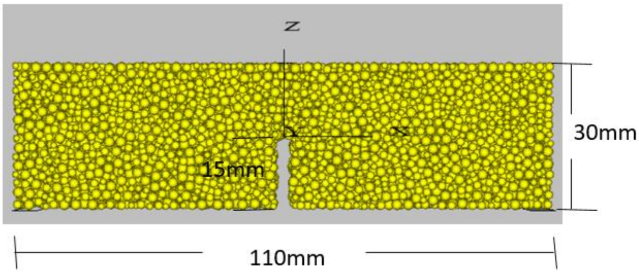

(a)

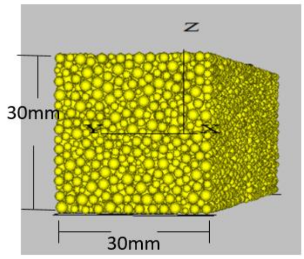

(b)

Fig. 3 A rectangular model in PFC3D

Fig. 2(b) also illustrates the displacement vector and bonding force distribution for the particles within the assembly. The experimental and numerical values of the tensile strength of the material in hand are shown in Table 2. These mechanical results demonstrating a good agreement and well matching in between the numerical and experimental results and validate the calibration procedure of PFC3D

2.3 model preparation using particle flow code

After calibration of PFC3D, three point bending test were simulated by creating a rectangular model in PFC3D (by using the calibrated micro-parameters) (Fig. 3). The PFC specimen had dimension of 30 mm×30 mm×110 mm (Fig. 3). minimum diameter of balls changes in 18 different models i.e., 0.55 mm (Fig. 4(a)), 0.65 mm(Fig. 4(b)), 0.75 mm(Fig. 4(c)), 0.85 mm(Fig. 4(d)), 0.95 mm(Fig. 4(e)), 1.05 mm(Fig. 4(f)), 1.15 mm(Fig. 4(g)), 1.25 mm(Fig.

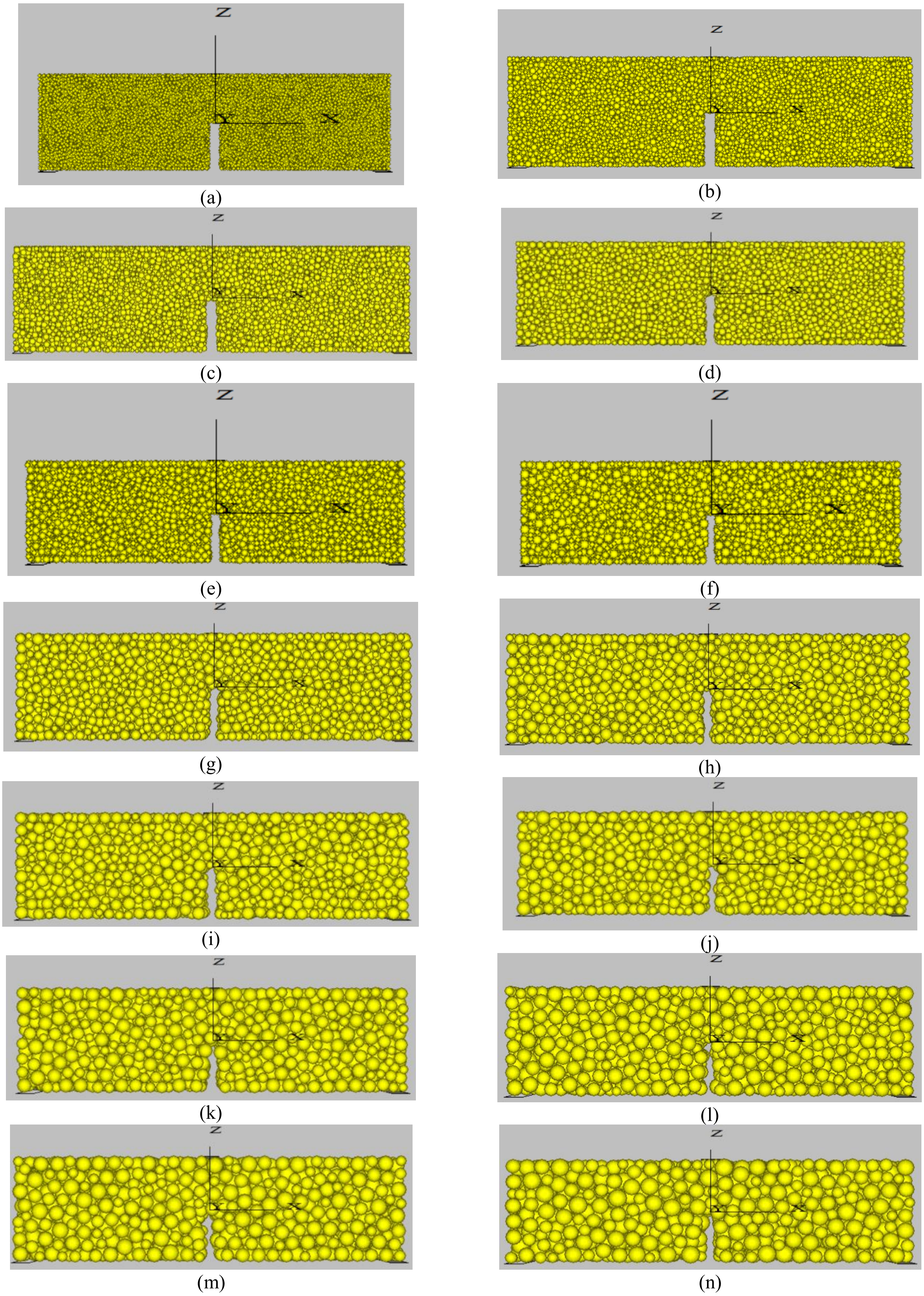

Fig. 4 The single edge-notched rectangle bar in bending (SENRBB) specimen with different ball radius of, (a) 0.55 mm, (b) 0.65 mm, (c) 0.75 mm, (d) 0.85 mm, (e) 0.95 mm, (f) 1.05 mm (g)1.15 mm, (h) 1.25 mm, (i) 1.35 mm, (j) 1.45 mm, (k) 1.55 mm, (l) 1.65 mm, (m)1.75 mm, (n) 1.85

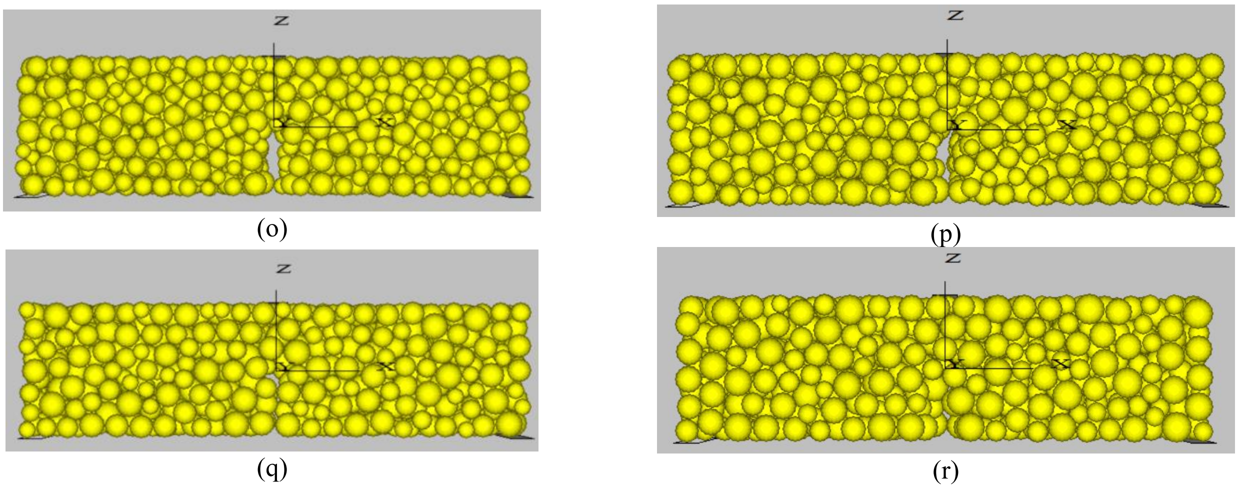

Fig. 4 Continued, (o)1.95 mm, (p) 2.05 mm, (q) 2.15 mm, (r) 2.25 mm

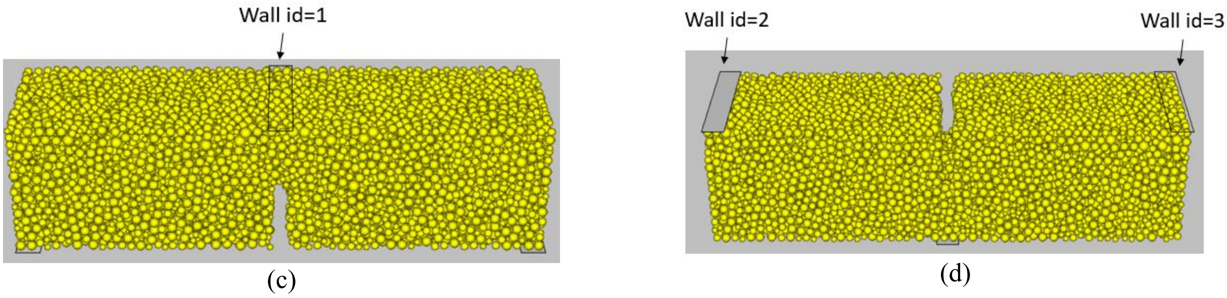

Fig. 5 Wall configuration in the single edge-notched rectangle bar

4(h)), 1.35 mm(Fig. 4(i)), 1.45 mm(Fig. 4(j)), 1.55 mm(Fig. 4(k)), 1.65 mm(Fig. 4(l)), 1.75 mm(Fig. 4 m)), 1.85 mm(Fig. 4(n)), 1.95 mm(Fig. 4(o)), 2.05 mm(Fig. 4(p)), 2.15 mm(Fig. 4(q)) and 2.25 mm(Fig. 4(r)). totally, 18 models consisting various ball number has been built, i.e., 55343 balls, 38495 balls, 22383 balls, 18273 balls, 11104 balls, 8157 balls, 6029 balls, 4834 balls, 3838 balls, 3097 balls, 2535 balls, 2102 balls, 1761 balls, 1491 balls, 1273 balls, 1096 balls, 950 balls and 829 balls. The ball size and ball number were listed in Table 3.

These models are loaded by three loading walls (Fig. 5). The Tensile force was registered by taking the reaction forces on the wall id=1.

3. Numerical results

3.1 The effect of particle size on the failure pattern of specimens

Figs. 6(a)-(r) shows the effect of particle size on the failure pattern of models with number of balls of 55343 balls, 38495 balls, 22383 balls, 18273 balls, 11104 balls, 8157 balls, 6029 balls, 4834 balls, 3838 balls, 3097 balls, 2535 balls, 2102 balls, 1761 balls, 1491 balls, 1273 balls, 1096 balls, 950 balls and 829 balls, respectively. Black line and red line show the tensile crack and shear crack, respectively. Failure pattern is constant by increasing the ball diameter. Tensile cracks are dominant mode of failure. These crack initiates from notch tip, propagate parallel to loading axis and coalescence with upper model boundary. It's to be note that number of cracks increase by decreasing the ball diameter.

3.2 The effect of particle size on the tensile fracture toughness

Tensile fracture toughness was measured by using Eqs. (1) and (2). Fig. 7 shows the effect of particle size on the tensile fracture toughness. The results show that tensile fracture toughness was decreased with increasing the particle size.

4. Conclusions

In this work the effect of particle size on the failure pattern and tensile fracture toughness in SENRBB specimen has been investigated using PFC3D. Firstly calibration of PFC3D was performed using Brazilian tensile strength. Secondly SENRBB test models consisting different particle size was simulated numerically. The results show that:

- Failure pattern is constant by increasing the ball diameter.
- Tensile cracks are dominant mode of failure.
- These crack initiates from notch tip, propagate parallel to loading axis and coalescence with upper model boundary.
- Number of cracks increase by decreasing the ball diameter.
- Tensile fracture toughness was decreased with

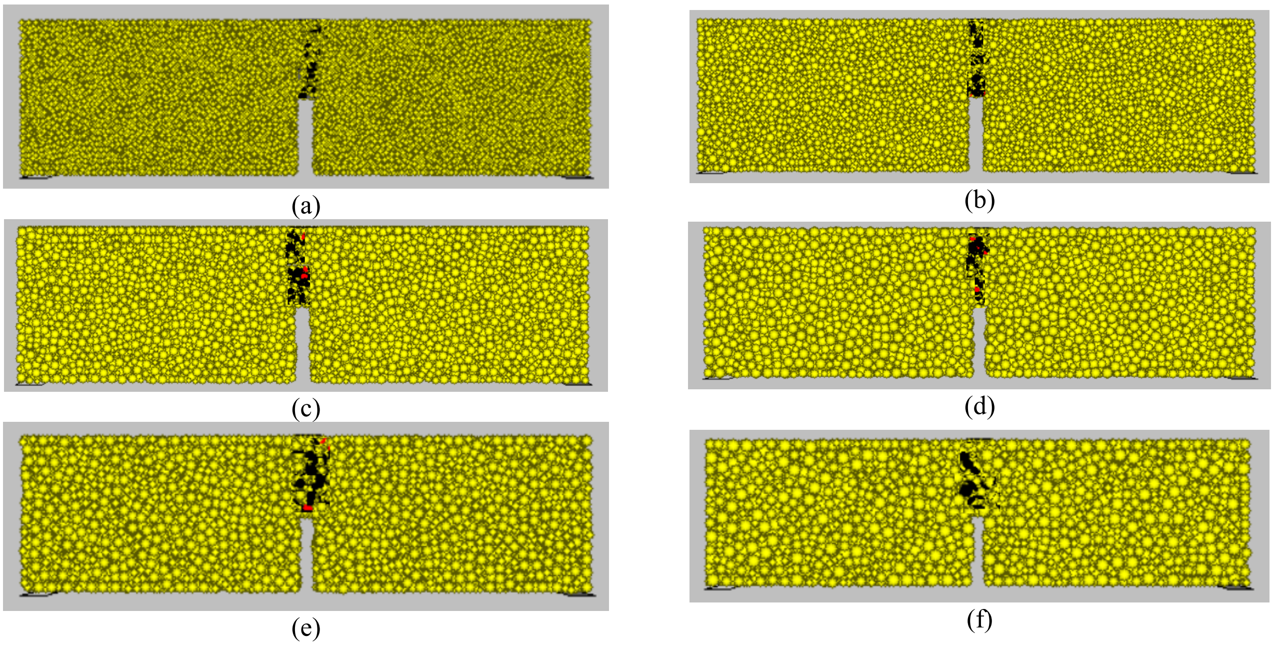

Fig. 6 Failure pattern in the single edge-notched rectangle bar with different ball radius of, (a) 0.55 mm, (b) 0.65 mm, (c) 0.75 mm, (d) 0.85 mm, (e) 0.95 mm, (f) 1.05 mm

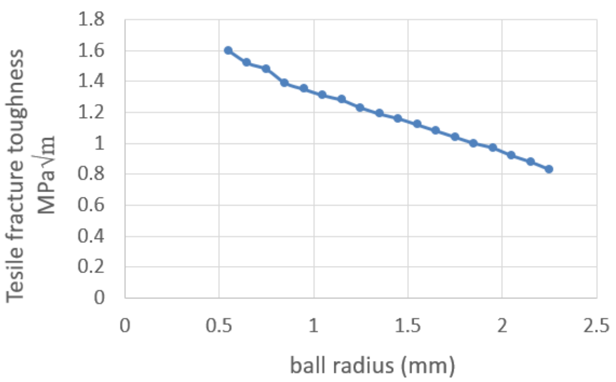

Fig. 7 The effect of particle size on the tensile fracture toughness

increasing the particle size.

References

Akbas S, (2016), "Analytical solutions for static bending of edge cracked micro beams", *Struct. Eng. Mech.*, **59**(3), 66-78.

Ameen, M., Raghu Prasad, B.K. and Gopalakrishnan, A.R. (2011), "Modeling of concrete cracking-a hybrid technique of using displacement discontinuity element method and direct boundary element method", *Eng. Analy. Bound. Elem.*, **35**(9), 1054-1059.

Belytschko, T. and Black, T. (1999), "Elastic crack growth in finite elements with minimal remeshing", *Int. J. Numer. Meth. Eng.*, **45**(5), 601-620.

Bi, J., Zhou, X.P. and Qian, Q.H. (2016), "The 3D Numerical simulation for the propagation process of multiple pre-existing flaws in rock-like materials subjected to biaxial compressive loads", *Rock Mech. Rock Eng.*, **49**(5), 1611-1627.

Bi, J., Zhou, X.P. and Xu, X.M. (2017), "Numerical simulation of failure process of rock-like materials subjected to impact loads", *Int. J. Geomech.*, **17**(3), 04016073

Bobet, A. (2000), "The initiation of secondary cracks in compression", *Eng. Fract. Mech.*, **66**(2), 187-219.

Bombolakis, E.G. (1968), "Photoelastic study of initial stages of brittle fracture in compression", *Tectonophys.*, **6**(6), 461-473.

Cundall, P.A. and Strack, O.D.L. (1979), "A discrete numerical model for granular assemblies", *Geotech.*, **29**(1), 47-65.

Donze, F.V., Richefeu, V. and Magnier, S.A. (2009), "Advances in discrete element method applied to soil rock and concrete mechanics", *Electr. J. Geol. Eng.*, **8**(1), 1-44.

Erdogan, F. and Sih, G.C. (1963), "On the crack extension path in plates under plane loading and transverse shear", *ASME J. Bas. Eng.*, **85**(4), 519-527.

Fan, Y., Zhu, Z., Kang, J. and Fu, Y. (2016), "The mutual effects between two unequal collinear cracks under compression", *Math. Mech. Sol.*, **22**, 1205-1218.

Freund, L.B. (1973), "Crack propagation in elastic solid subjected to general loading. Stress wave loading", *J. Mech. Phys. Sol.*, **21**(2), 47-61.

Gerges, N., Issa, C. and Fawaz, S. (2015), "Effect of construction joints on the splitting tensile strength of concrete", *Case Stud. Constr. Mater.*, **3**, 83-91.

Ghazvinian, A., Sarfarazi, V., Schubert, W. and Blumel, M. (2012), "A study of the failure mechanism of planar nonpersistent open joints using PFC2D", *Rock Mech. Rock Eng.*, **45**(5), 677-693.

Haeri, H. (2015b), "Propagation mechanism of neighboring cracks in rock-like cylindrical specimens under uniaxial compression", *J. Min. Sci.*, **51**(3), 487-496.

Haeri, H., Sarfarazi, V., Fatehi, M., Hedayat, A. and Zhu, Z. (2016c), "Experimental and numerical study of shear fracture in brittle materials with interference of initial double", *Acta Mech. Soild. Sinic.*, **5**, 555-566.

Haeri, H. (2015a), "Influence of the inclined edge notches on the shear-fracture behavior in edge-notched beam specimens", *Comput. Concrete*, **16**(4), 605-623.

Haeri, H. (2016), "Propagation mechanism of neighboring cracks in rock-like cylindrical specimens under uniaxial compression", *J. Min. Sci.*, **51**(5), 1062-1106.

Haeri, H. 2015c, "Influence of the inclined edge notches on the shear-fracture behavior in edge-notched beam specimens", *Comput. Concrete*, **16**, 605-623.

Haeri, H., Khaloo, A. and Marji, M.F. (2015a), "Experimental and numerical simulation of the microcrack coalescence mechanism in rock-like materials", *Strength Mater*., **47**(5), 740-754.

Haeri, H., Khaloo, A. and Marji, M.F. (2015b), "Fracture analyses of different pre-holed concrete specimens under compression", *Acta Mech*. *Sinic*., **31**(6), 855-870.

Haeri, H., Khaloo, A. and Marji, M.F. (2015c), "A coupled experimental and numerical simulation of rock slope joints behavior", *Arab*. *J. Geosci*., **8**(9), 7297-7308.

Haeri, H., Sarfarazi, V. and Hedayat, A. (2016a), "Suggesting a new testing device for determination of tensile strength of concrete", *Struct*. *Eng*. *Mech*., **60**(6), 939-952.

Haeri, H., Sarfarazi, V. and Lazemi, H. (2016b), "Experimental study of shear behavior of planar non-persistent joint", *Comput*. *Concrete*, **17**(5), 639-653.

Haeri, H. and Sarfarazi, V. (2016), "The effect of non-persistent joints on sliding direction of rock slopes", *Comput. Concrete*, **17**(6),723-737

Haeri, H., Shahriar, K. and Marji, M.F. (2013), "Modeling the propagation mechanism of two random micro cracks in rock samples under uniform tensile loading,", *Proceedings of the ICF13*.

Haeri, H., Shahriar, K., Fatehi Marji, M. and Moarefvand, P. (2014), "On the crack propagation analysis of rock like Brazilian disc specimens containing cracks under compressive line loading", *Lat*. *Am*. *J*. *Sol*. *Struct*., **11**(8), 1400-1416.

Hoek, E. and Bieniawski, Z.T. (1965), "Brittle fracture propagation in rock under compression", *Int*. *J*. *Fract*., **1**(3), 137-155.

Hofmann H., Babadagli T., Yoon J. S., Zang A. and Zimmermann G. (2015), "A grain based modeling study of mineralogical factors affecting strength, elastic behavior and micro fracture development during compression tests in granites", *Eng*. *Fract*. *Mech*., **147**, 261-275.

Hussian, M.A., Pu, E.L. and Underwood, J.H. (1974), *Strain Energy Release Rate for a Crack under Combined Mode I and Mode II. In: Fracture Analysis, ASTM STP 560,* American Society for Testing and Materials, 2-28.

Ingraffea, A.R. and Heuze, F.E. (1980), "Finite element models for rock fracture mechanics", *Int*. *J*. *Numer*. *Analy*. *Meth*. *Geomech*., **4**(1), 25-43.

Itasca, C.G. (2002), *Users' Manual for Particle Flow Code in 2 Dimensions (PFC2D)*, Version 3.1, Minneapolis, Minnesota, U.S.A.

Itou, S. (1996), "Dynamic stress intensity factors of two collinear cracks in orthotropic medium subjected to time-harmonic disturbance", *Theoret*. *Appl*. *Fract*. *Mech*., **25**(2), 155-166.

Janeiro, R.P. and Einstein, H.H. (2010), "Experimental study of the cracking behavior of specimens containing inclusions (under uniaxial compression)", *Int*. *J*. *Fract*., **164**(1), 83-102.

Jiang, Z., Wan, S., Zhong, Z., Li, M. and Shen, K. (2014), "Determination of mode-I fracture toughness and nonuniformity for GFRP double cantilever beam specimens with an adhesive layer", *Eng*. *Fract*. *Mech*., **128**, 139-156.

Jiefan, H., Ganglin, C., Yonghong, Z. and Ren, W. (1990), "An experimental study of the strain field development prior to failure of a marble plate under compression", *Tectonophys*., **175**(1-3), 184-269.

Lajtai, E.Z. (1971), "A theoretical and experimental evaluation of the Griffith theory of brittle fracture", *Tectonophys*., **11**(2), 129-156.

Lajtai, E.Z. (1974), "Brittle fractures in compression", *Int*. *J*. *Fract*., **10**(4), 525-536.

Lancaster, I.M., Khalid, H.A. and Kougioumtzoglou, I.A. (2013), "Extended FEM modelling of crack propagation using the semicircular bending test", *Constr*. *Build*. *Mater*., **48**, 270-277.

Lee, S. and Chang, Y. (2015), "Evaluation of RPV according to alternative fracture toughness requirements", *Struct*. *Eng*. *Mech*., **53**(6).

Leonel, E.D., Chateauneuf, A. and Venturini, W.S. (2012), "Probabilistic crack growth analyses using a boundary element model: Applications in linear elastic fracture and fatigue problems", *Eng*. *Analy*. *Bound*. *Elem*., **36**, 944-959.

Li, S., Wang, H., Li, Y., Li, Q., Zhang, B. and Zhu, H. (2016), "A new mini-grating absolute displacement measuring system for static and dynamic geomechanical model tests", *Measure*., **82**, 421-431.

Li, Y.P., Chen, L.Z. and Wang, Y.H. (2005), "Experimental research on pre-cracked marble under compression", *Int*. *J*. *Sol*. *Struct*., **42**, 2505-2516.

Lin, C.H. and Lin, M.L. (2015), "Evolution of the large landslide induced by Typhoon Morakot: A case study in the Butangbunasi River, Southern Taiwan using the discrete element method", *Eng*. *Geol*., **197**, 172-187.

Liu, X., Nie, Z., Wu, S. and Wang, C. (2015), "Self-monitoring application of conductive asphalt concrete under indirect tensile deformation", *Case Stud*. *Constr*. *Mater*., **3**, 70-77.

Lu, F.Y., Lin, Y.L., Wang, X.Y., Lu, L. and Chen, R. (2015), "A theoretical analysis about the influence of interfacial friction in SHPB tests", *Int*. *J*. *Imp*. *Eng*., **79**, 95-101.

Miller, J.T. and Einstein, H.H. (2008), "Crack coalescence tests on granite", *Proceedings of the 42nd US Rock Mechanics Symposium,* San Francisco, U.S.A.

Mobasher, B., Bakhshi, M. and Barsby, C. (2014), "Backcalculation of residual tensile strength of regular and high performance fibre reinforced concrete from flexural tests", *Constr*. *Build*. *Mater*., **70**, 243-253.

Mohammad, A. (2016), "Statistical flexural toughness modeling of ultra-high performance mortar using response surface method", *Comput*. *Concrete*, **17**(4), 33-39.

Mughieda, O. and Alzoubi, A.K. (2004), "Fracture mechanisms of offset rock joints-a laboratory investigation", *Geotech*. *Geol*. *Eng*., **22**(4), 545-562.

Noel, M. and Soudki, K. (2014), "Estimation of the crack width and deformation of FRP-reinforced concrete flexural members with and without transverse shear reinforcement", *Eng*. *Struct*., **59**, 393-398.

Oetomo, J.J., Vincens, E., Dedecker, F. and Morel, J.C. (2016), "Modeling the 2D behavior of dry-stone retaining walls by a fully discrete element method", *Int*. *J*. *Numer*. *Analy*. *Meth*. *Geomech*., **40**(7), 1099-1120.

Oliveira, H.L. and Leonel, E.D. (2014), "An alternative BEM formulation, based on dipoles of stresses and tangent operator technique, applied to cohesive crack growth modeling", *Eng*. *Analy*. *Bound*. *Elem*., **41**, 74-82.

Ozecebe, G. (2011), "Minimum flexural reinforcement for Tbeams made of higher strength concrete", *Can*. *J*. *Civil Eng*., **26**(5), 525-534.

Pan, B., Gao, Y. and Zhong, Y. (2014), "Theoretical analysis of overlay resisting crack propagation in old cement mortar pavement", *Struct*. *Eng*. *Mech*., **52**(4) 167-181.

Park, N.S. (2001), "Crack propagation and coalescence in rock under uniaxial compression", M.Sc. Dissertation, Seoul National University, Korea.

Potyondy, D.O. and Cundall, P.A. (2004), "A bonded-particle model for rock", *Int*. *J*. *Rock Mech*. *Min*. *Sci*., **41**, 1329-1364.

Rajabi, M., Soltani, N. and Eshraghi, I. (2016), "Effects of temperature dependent material properties on mixed mode crack tip parameters of functionally graded materials", *Struct*. *Eng*. *Mech*., **58**(2), 144-156.

Ramadoss, P. and Nagamani, K. (2013), "Stress-strain behavior and toughness of high-performance steel fiber reinforced mortar in compression", *Comput*. *Mortar*, **11**(2), 55-65.

Reyes, O. and Einstein, H.H. (1991), "Failure mechanisms of

fractured rock-a fracture coalescence model", *Proceedings of the 7th Congress of the ISRM*, Aachen, Germany.
Ruiz, G. and Carmona, R.J. (2006a), "Experimental study on the influence of the shape of the cross-section and the rebar arrangement on the fracture of LRC beams", *Mater. Struct.*, **39**(3), 343-352.
Ruiz, G., Carmona, R.J. and Cendon, D.A. (2006b), "Propagation of a cohesive crack through adherent reinforcement layers", *Comput. Meth. Appl. Mech. Eng.*, **195**(52), 7237-7248.
Sagong, M. and Bobet, A. (2002), "Coalescence of multiple flaws in a rock-model material in uniaxial compression", *Int. J. Rock Mech. Min. Sci.*, **39**(2), 229-241.
Sardemir, M. (2016), "Empirical modeling of flexural and splitting tensile strengths of concrete containing fly ash by GEP", *Comput. Concrete*, **17**(4), 489-498.
Sarfarazi, V. and Haeri, H. (2016), "Effect of number and configuration of bridges on shear properties of sliding surface", *J. Min. Sci.*, **52**(2), 245-257.
Sarfarazi, V. and Haeri, H. (2016c), "A review of experimental and numerical investigations about crack propagation", *Comput. Concrete*, **18**(2), 235-266.
Sarfarazi, V. and Shubert, W. (2016b), "Numerical simulation of tensile failure of concrete in direct, flexural, double punch tensile and ring tests", *Period. Polyech. Civil Eng.*, **2**, 1-8.
Sarfarazi, V., Faridi, H.R., Haeri, H. and Schubert, W. (2016c), "A new approach for measurement of anisotropic tensile strength of concrete", *Adv. Concrete Constr.*, **3**(4), 269-284.
Sarfarazi, V., Ghazvinian, A., Schubert, W., Blumel, M. and Nejati, H.R. (2014), "Numerical simulation of the process of fracture of echelon rock joints", *Rock Mech. Rock Eng.*, **47**(4), 1355-1371.
Sarfarazi, V., Haeri, H. and Khaloo, A. (2016a), "The effect of non-persistent joints on sliding direction of rock slopes", *Comput. Concrete*, **17**(6), 723-737.
Shaowei, H., Aiqing, X., Xin, H. and Yangyang, Y. (2016), "Study on fracture characteristics of reinforced concrete wedge splitting tests", *Comput. Concrete*, **18**(3), 337-354.
Shen, B. (1995), "The mechanism of fracture coalescence in compression-experimental study and numerical simulation", *Eng. Fract. Mech.*, **51**(1), 73-85.
Shen, B. and Stephansson, O. (1994), "Modification of the Gcriterion for crack propagation subjected to compression", *Eng. Fract. Mech.*, **47**(2), 177-189.
Shuraim, A.B., Aslam, F., Hussain, R. and Alhozaimy, A. (2016), "Analysis of punching shear in high strength RC panels-experiments, comparison with codes and FEM results", *Comput. Concrete*, **17**(6), 739-760.
Sih, G.C. (1974), "Strain-energy-density factor applied to mixed mode crack problems", *Int. J. Fract.*, **10**(3), 305-321.
Silling, S.A. (2000), "Reformulation of elasticity theory for discontinuities and long-range forces", *J. Phys. Sol.*, **48**(1), 175209.
Silling, S.A. (2017), "Stability of peridynamic correspondence material models and their particle discretizations", *Comput. Meth. Appl. Mech. Eng.*, **322**, 42-57.
Silva, R.V., Brito, J. and Dhir, R.K. (2015), "Tensil strength behaviour of recycled aggregate concrete", *Constr. Build. Mater.*, **83**, 108-118.
Tang, C.A. and Kou, S.Q. (1998), "Crack propagation and coalescence in brittle materials under compression", *Eng. Fract. Mech.*, **61**(3-4), 311-324.
Tang, C.A., Lin, P., Wong, R.H.C. and Chau, K.T. (2001), "Analysis of crack coalescence in rock-like materials containing three flaws-part II: Numerical approach", *Int. J. Rock Mech. Min. Sci.*, **38**(7), 925-939.
Tiang, Y., Shi, S., Jia, K. and Hu, S. (2015), "Mechanical and dynamic properties of high strength concrete modified with lightweight aggregates presaturated polymer emulsion", *Constr. Build. Mater.*, **93**, 1151-1156.
Vallejo, L.E. (1987), "The influence of fissures in a stiff clay subjected to direct shear", *Geotech.*, **37**(1), 69-82.
Vallejo, L.E. (1988), "The brittle and ductile behavior of clay samples containing a crack under mixed mode loading", *Theoret. Appl. Fract. Mech.*, **10**(1), 73-78.
Vásárhelyi, B. and Bobet, A. (2000), "Modeling of crack initiation, propagation and coalescence in uniaxial compression", *Rock Mech. Rock Eng.*, **33**(2), 119-139.
Vesga, L.F., Vallejo, L.E. and Lobo-Guerrero, S. (2008), "DEM analysis of the crack propagation in brittle clays under uniaxial compression tests", *Int. J. Numer. Analy. Meth. Geomech.*, **32**(11), 1405-1415.
Wang, R., Zhao, Y., Chen, Y., Yan, H., Yin, Y.Q., Yao, C.Y. and Zhang, H. (1987), "Experimental and finite simulation of Xshear fractures from a crack in marble", *Tectonophys.*, **144**, 141150.
Wang, T., Dai, J.G. and Zheng, J.J. (2015), "Multi-angle truss model for predicting the shear deformation of RC beams with low span-effective depth ratios", *Eng. Struct.*, **91**, 85-95.
Wang, X., Zhu, Z., Wang, M., Ying, P., Zhou, L. and Dong, Y. (2017), "Study of rock dynamic fracture toughness by using VB-SCSC specimens under medium-low speed impacts", *Eng. Fract. Mech.*, **181**, 52-64.
Wong, L.N.Y. and Einstein, H.H. (2008a), "Crack coalescence in molded gypsum and Carrara marble: Part 1. Macroscopic observations and interpretation", *Rock Mech. Rock Eng.*, **42**(3), 475-511.
Wong, L.N.Y. and Einstein, H.H. (2008b), "Crack coalescence in molded gypsum and Carrara marble: Part 2. Microscopic observations and interpretation", *Rock Mech. Rock Eng.*, **42**(3), 513-545.
Wong, L.N.Y. and Einstein, H.H. (2009), "Systematic evaluation of cracking behavior in specimens containing single flaws under uniaxial compression", *Int. J. Rock Mech. Min. Sci.*, **46**(2), 239249.
Wong, R.H.C. and Chau, K.T. (1998), "Crack coalescence in a rock-like material containing two cracks", *Int. J. Rock Mech. Min. Sci.*, **35**(2), 147-164.
Wong, R.H.C., Chau, K.T., Tang, C.A. and Lin, P. (2001), "Analysis of crack coalescence in rock-like materials containing three flaws-part I: Experimental approach", *Int. J. Rock Mech. Min. Sci.*, **38**(7), 909-924.
Wong, R.H.C., Guo, Y.S.H., Liu, L.Q., Liu, P.X. and Ma, S.P. (2008), "Nucleation and growth of anti-wing crack from tips of strike-slip flaw", *Proceedings of the 42nd US Rock Mechanics Symposium*, San Francisco, U.S.A.
Yang, S.Q. (2015), "An experimental study on fracture coalescence characteristics of brittle sandstone specimens combined various flaws", *Geomech. Eng.*, **8**(4), 541-557.
Yaylac, M. (2016), "The investigation crack problem through numerical analysis", *Struct. Eng. Mech.*, **57**(6).
Yoshihara, H. (2013), "Initiation and propagation fracture toughness of solid wood under the mixed mode I/II condition examined by mixed-mode bending test", *Eng. Fract. Mech.*, **104**, 1-15.
Zeng, G., Yang, X., Yina, A. and Bai, F. (2014), "Simulation of damage evolution and crack propagation in three-point bending pre-cracked asphalt mixture beam", *Constr. Build. Mater.*, **55**, 323-332.
Zhang, Q., Zhu, H.H. and Zhang, L. (2015), "Studying the effect of non-spherical microparticles on Hoek-Brown strength parameter mi using numerical true triaxial compressive tests", *Int. J. Numer. Analy. Meth. Geomech.*, **39**(1), 96-114.
Zhao, Y., Zhao, G.F. and Jiang, Y. (2013), "Experimental and numerical modelling investigation on fracturing in coal under

impact loads", *Int. J. Fract.*, **183**(1), 63-80.

Zhou, M. and Song, E. (2016), "A random virtual crack DEM model for creep behavior of rockfll based on the subcritical crack propagation theory", *Acta Geotech.*, **11**(4), 827-847.

Zhou, X.P., Xia, E.M., Yang, H.Q. and Qian, Q.H. (2012), "Different crack sizes analyzed for surrounding rock mass around underground caverns in Jinping I hydropower station", *Theoret. Appl. Fract. Mech.*, **57**(1), 19-30.

Zhou, X.P. and Yang, H.Q. (2007), "Micromechanical modeling of dynamic compressive responses of mesoscopic heterogenous brittle rock", *Theoret. Appl. Fract. Mech.*, **48**(1), 1-20.

Zhou, X.P., Zhang, Y.X. and Ha, Q.L. (2008), "Real-time computerized tomography (CT) experiments on limestone damage evolution during unloading", *Theoret. Appl. Fract. Mech.*, **50**(1), 49-56.

Zhou, X.P. (2004), "Analysis of the localization of deformation and the complete stress-strain relation for mesoscopic heterogeneous brittle rock under dynamic uniaxial tensile loading", *Int. J. Sol. Struct.*, **41**(5/6), 1725-1738.

Zhou, X.P., Ha, Q., Zhang, Y. and Zhu, K. (2004), "Analysis of deformation localization and the complete stress-strain relation for brittle rock subjected to dynamic compressive loads", *Int. J. Rock Mech. Min. Sci.*, **41**(2), 311-319.

Zhou, X.P., Shou, Y.D., Qian, Q.H. and Yu, M.H. (2014), "Three-dimensional nonlinear strength criterion for rock-like materials based on the micromechanical method", *Int. J. Rock Mech. Min. Sci.*, **72**, 54-60.

Zhou, X.P. and Wang, Y.T. (2016), "Numerical simulation of crack propagation and coalescence in pre-cracked rock-like Brazilian disks using the non-ordinary state-based peridynamics", *Int. J. Rock Mech. Min. Sci.*, **89**, 235-249.

Zhou, X.P. and Yang, H.Q. (2012), "Multiscale numerical modeling of propagation and coalescence of multiple cracks in rock masses", *Int. J. Rock Mech. Min. Sci.*, **55**, 15-27.

Zhou, X.P., Bi, J. and Qian, Q.H. (2015), "Numerical simulation of crack growth and coalescence in rock-like materials containing multiple pre-existing flaws", *Rock Mech. Rock Eng.*, **48**(3), 1097-1114.

Zhou, X.P., Gu, X.B. and Wang, Y.T. (2015), "Numerical simulations of propagation, bifurcation and coalescence of cracks in rocks", *Int. J. Rock Mech. Min. Sci.*, **80**, 241-254.

CC